

# Testing the strong equivalence principle with the triple pulsar PSR J0337+1715

Lijing Shao\*

Max Planck Institute for Gravitational Physics (Albert Einstein Institute),  
Am Mühlenberg 1, D-14476 Potsdam-Golm, Germany

(Dated: March 16, 2016)

Three conceptually different masses appear in equations of motion for objects under gravity, namely, the inertial mass,  $m_{\mathcal{I}}$ , the passive gravitational mass,  $m_{\mathcal{P}}$ , and the active gravitational mass,  $m_{\mathcal{A}}$ . It is assumed that, for any objects,  $m_{\mathcal{I}} = m_{\mathcal{P}} = m_{\mathcal{A}}$  in the Newtonian gravity, and  $m_{\mathcal{I}} = m_{\mathcal{P}}$  in the Einsteinian gravity, oblivious to objects' sophisticated internal structure. Empirical examination of the equivalence probes deep into gravity theories. We study the possibility of carrying out new tests based on pulsar timing of the stellar triple system, PSR J0337+1715. Various machine-precision three-body simulations are performed, from which, the equivalence-violating parameters are extracted with Markov chain Monte Carlo sampling that takes full correlations into account. We show that the difference in masses could be probed to  $3 \times 10^{-8}$ , improving the current constraints from lunar laser ranging on the post-Newtonian parameters that govern violations of  $m_{\mathcal{P}} = m_{\mathcal{I}}$  and  $m_{\mathcal{A}} = m_{\mathcal{P}}$  by thousands and millions, respectively. The test of  $m_{\mathcal{P}} = m_{\mathcal{A}}$  would represent the first test of Newton's third law with compact objects.

## I. INTRODUCTION

Mass is an important concept whose notion has evolved dramatically during several important paradigm shifts in theoretical physics, from its original meaning of *amount*, to *inertia* in Newtonian mechanics, to *energy* in special relativity with the famous  $E = mc^2$  [1]. Mass was further developed by Einstein and Schwarzschild into an intimate relation with the geometry of spacetime in general relativity (GR) [2, 3]. In quantum world, mass pertains to an object's de Broglie relation and Compton wavelength in the nonrelativistic theory [4]. In relativistic field theories, the origin of mass results from spontaneous symmetry breaking with the Higgs field seeking a minimum point of potential [5, 6], which was verified at the LHC [7, 8]. From a group-theoretic viewpoint, mass is a Casimir invariant of the Poincaré group, hence labels the irreducible representations [9].

We here study the concept of mass with the classical gravitational interaction. In a theoretically independent way, there are three masses defined by measurement [10]: i) the inertial mass,  $m_{\mathcal{I}}$ , enters Newton's second law,  $\mathbf{F} = m_{\mathcal{I}}\mathbf{a}$ ; ii) the passive gravitational mass,  $m_{\mathcal{P}}$ , is the mass on which gravity acts, defined by  $\mathbf{F} = -m_{\mathcal{P}}\nabla U$ ; iii) the active gravitational mass,  $m_{\mathcal{A}}$ , is the mass that sources gravity, through the (integrated) Poisson's equation,  $\oint_{\partial V} \mathbf{g} \cdot d\mathbf{A} = -4\pi G m_{\mathcal{A}}$ . In the Newtonian gravity, these conceptually different masses are assumed to be equal, namely  $m_{\mathcal{I}} = m_{\mathcal{P}} = m_{\mathcal{A}}$ . In GR, the geometric foundation is built upon the equality of  $m_{\mathcal{I}}$  and  $m_{\mathcal{P}}$  (dubbed the equivalence principle [11]). The equality of  $m_{\mathcal{A}}$  with the other two is of debate in GR [12, 13]. While Bonnor found that, assuming  $m_{\mathcal{I}} = m_{\mathcal{P}}$ ,  $m_{\mathcal{A}}$  deviates by a few times from  $m_{\mathcal{P}}$  for a static sphere of uniform density under strong gravity [12], Rosen and Cooperstock

showed that there is only one mass for an isolated body when the gravitational energy is taken into account [13].

The importance of experimental examination of equivalence of masses was realized early in Newton's era [14]. High precision tests of the weak equivalence principle (i.e.,  $m_{\mathcal{I}} = m_{\mathcal{P}}$  for non-self-gravitating bodies) include pendulum experiments of Newton, Bessel, Potter, and torsion-balancing experiments of Eötvös, Dicke, Braginsky, Adelberger, et al. [15]. Recent developments are putting the test into space with missions like MICROSCOPE [16], Galileo-Galilei [17], and STEP [18]. In addition, lunar laser ranging (LLR) [19, 20] and pulsar timing [21–25] probed the equivalence principle with self-gravitating bodies and limited the Nordtvedt parameter [26],  $\eta_{\text{N}}$ , to be less than  $3 \times 10^{-4}$  and  $3 \times 10^{-2}$  respectively. In a vivid contrast, tests of the equality  $m_{\mathcal{P}} = m_{\mathcal{A}}$  are fewer. We only noticed two experiments,<sup>1</sup> one performed by Kreuzer using a Cavendish balance that limited the difference in  $m_{\mathcal{P}}/m_{\mathcal{A}}$  between fluorine and bromine to  $\lesssim 5 \times 10^{-5}$  [28], and the other performed by Bartlett and van Buren with LLR that limited the difference between iron and aluminum to  $\lesssim 4 \times 10^{-12}$  [29].

Here we propose new tests of equivalence of masses with the remarkable stellar triple system, PSR J0337+1715 [30]. Various machine-precision three-body simulations are performed closely following observational characteristics. Possible violations in the equivalence of masses are *injected* directly via equations of motion [31], and recovered with a dedicated Markov chain Monte Carlo (MCMC) sampler taking full correlations into account. Our results suggest that the triple system has sensitivity  $\sim 3 \times 10^{-8}$  to probe the difference in masses. It could improve the current post-Newtonian limits by thousands for  $m_{\mathcal{I}} = m_{\mathcal{P}}$  and millions for

<sup>1</sup> In addition, Nordtvedt had a proposal to test  $m_{\mathcal{A}} = m_{\mathcal{P}}$  by utilizing the Earth's south-north asymmetric distribution of ocean water [27]; but no subsequent analysis is published.

\* lshao@aei.mpg.de

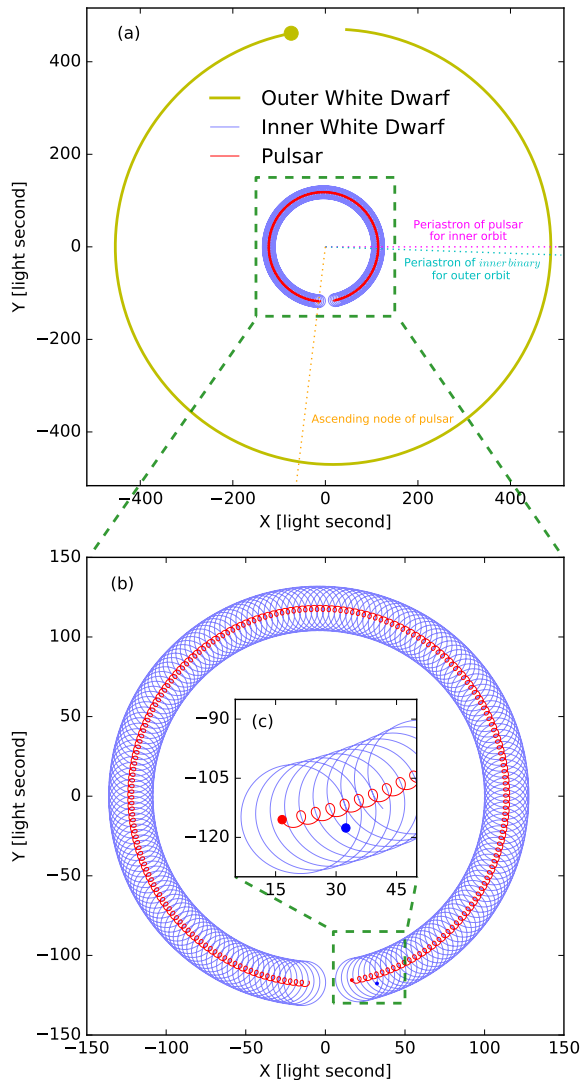


FIG. 1. Illustration of the triple system, projected on the orbital plane of the *inner binary*. In (a) dotted lines mark directions of the periastron of the pulsar for the inner orbit, the periastron of *inner binary* for the outer orbit, and the ascending node of the pulsar; in Figure 2 of Ref. [30], these directions are indicated for WDs. (b) and (c) are magnified views of the regions enclosed by the green dashed boxes. These trajectories start on MJD 55920.0 (December 25, 2011), and end on MJD 56233.9 (November 2, 2012). The starting locations are indicated by dots.

$m_{\mathcal{A}} = m_{\mathcal{P}}$ , and would represent the first test of Newton’s third law with compact objects.

## II. THE TRIPLE SYSTEM

PSR J0337+1715 is a triple system consisting of a neutron star (NS) with mass  $1.44 M_{\odot}$  and two white dwarfs (WDs) with masses  $0.20 M_{\odot}$  and  $0.41 M_{\odot}$  [30, 32]. The NS and the lighter WD are gravitationally bound as an

*inner binary* with  $P_{b,I} = 1.63$  d that are, as a whole, hierarchically bound to the outer WD with  $P_{b,O} = 327$  d. Two orbits are very circular with  $e_I = 6.9 \times 10^{-4}$  for the *inner binary*, and  $e_O = 3.5 \times 10^{-2}$  for the outer orbit. Two orbital planes are remarkably coplanar with an inclination  $\lesssim 0.01^{\circ}$  [30].

An illustration of orbits is given in Figure 1. It was simulated with the parameters reported in Ref. [30]. Initial conditions are worked out for MJD 55920.0 which is the reference epoch for all parameters. The three-body evolution under Newtonian gravity is performed with the IAS15 integrator in REBOUND<sup>2</sup> [33]. The IAS15 integrator is a 15th-order integrator based on the Gauß-Radau quadrature. It uses adaptive time stepping, and keeps systematic errors well below machine precision over  $10^9$  orbits [34]. The precision is very important for three-body dynamics, because the pulsar timing experiments spanning  $\sim 1.4$  yr ( $\sim 4 \times 10^7$  s) have achieved a weighted RMS residual,  $\sigma_{\text{TOA}} = 1.34 \mu\text{s}$  [30]. Our numerical integration has to be more accurate than that in order to study tiny effects in the orbital dynamics.

## III. PULSAR TIMING AND PARAMETER ESTIMATION

We evolve the triple system in 3D for a longer time than the observation in Ref. [30], and then cut data keeping the part which corresponds to the real data span (MJD 55930.9—56436.5). A spin-down model for the pulsar,  $f(t) = f_0 + \dot{f}t$ , is constructed with a spin frequency,  $f_0 = 365.953363096$  Hz, and its first time derivative,  $\dot{f} = -2.3658 \times 10^{-15}$  Hz s<sup>-1</sup>. By projecting the pulsar’s trajectory along its line of sight to the Earth, we obtain the geometric delay of pulse signals (i.e., the Römer delay). Together with the spin-down model, simulated times of arrival (TOAs),  $N(t)$ , with  $N$  the counting number of pulses and  $t$  the coordinate time, are recorded. Relativistic effects (e.g., the periastron advance, the gravitational damping, the Shapiro time delay) are not observable in practice yet [30], therefore not included. The only exception is the transverse Doppler effect due to the cross term of velocities for inner and outer orbits [30]. It is approximated as  $R(t) \simeq \int \frac{1}{c^2} \mathbf{v}_O \cdot \mathbf{v}_I dt = \frac{1}{c^2} \mathbf{x}_I(t) \cdot \mathbf{v}_O(t) - \int \frac{1}{c^2} \mathbf{x}_I \cdot d\mathbf{v}_O \simeq \frac{1}{c^2} \mathbf{x}_I(t) \cdot \mathbf{v}_O(t)$ , where constants and the integral term, which is smaller by a factor  $\sim P_{b,I}/P_{b,O}$  on the timescale of the inner orbit, are dropped [35].  $R(t)$  has an amplitude  $\sim 50 \mu\text{s}$ , consistent with the real data [30]. 26280 TOAs are sampled from our simulation either uniformly in time (*uniform sampling* hereafter) or with fake observing blocks once a week with TOAs being separated by 10 seconds within block (*step sampling*). A Gaussian noise with a variance  $\sigma_{\text{TOA}} = 1.34 \mu\text{s}$  is added homogeneously to TOAs

<sup>2</sup> <https://github.com/hannorein/rebound>

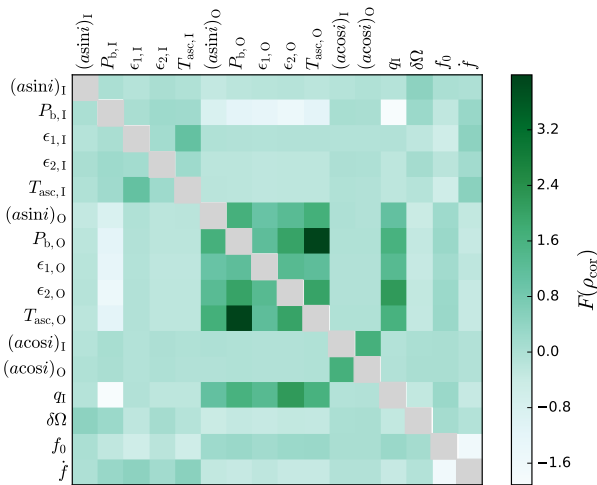


FIG. 2. The correlations between 16 fitting parameters.  $F(\rho_{\text{cor}}) \equiv \log_{10}[(1+\rho_{\text{cor}})/(1-\rho_{\text{cor}})] - \rho_{\text{cor}} \log_{10} 2$  is a function defined such that it counts 9's in the limit of large correlations [e.g.,  $F(0.999) \simeq +3$ ,  $F(-0.9) \simeq -1$ , and  $F(0) = 0$ ]; on diagonal,  $F(\rho_{\text{cor}})$  diverges.

to mimic the observation uncertainty [30]. Several noise realizations are simulated for each sampling method.

Following the method in Ref. [30], we set up MCMC runs to estimate parameters. To follow the fitting of real data as closely as possible, the same set of parameters are used, which include 2 parameters for the pulsar's spin-down, and 14 parameters for the size, the shape, the orientation, and the initial condition of two orbits (details can be found in Ref. [30]). The PYTHON implementation of an affine-invariant MCMC ensemble sampler [36, 37], EMCEE,<sup>3</sup> is used to explore the 16D parameter space. In each step, we generate noiseless template TOAs according to 16 parameters that are being sampled by the kernel. They are compared with the TOAs generated before. The runs proceed the exploration of parameter space according to the difference between two sets of TOAs, characterized by  $\chi^2$  (for details of the Markov-chain implementation, see Ref. [37]).

We accumulate 320000 MCMC samples for each set of simulated TOAs, of which the first half are abandoned as the BURN-IN phase [38]. The Gelman-Rubin statistic is used to verify the convergence of different chains [39]. The 16D parameter space is marginalized to obtain the uncertainty for each parameter. It is remarkable that with the only input of the orbital characteristics and a timing noise, we recover all observational *uncertainties* for 14 orbital parameters [30] within a factor of 2, except the difference in the longitude of ascending nodes for two orbits, whose uncertainty is off by a factor of 3. Uncertainties of the spin-down parameters are however underestimated, by factors of 4000 for  $f_0$  and 10 for  $\dot{f}$ , which

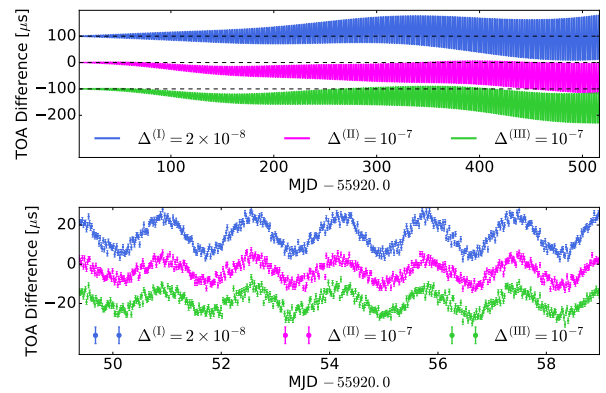


FIG. 3. The difference in simulated TOAs introduced by hypothetical violations in the equivalence of masses. Lower panel is a magnified view of a small region that contains 6 inner orbits. The blue and green series are offset vertically for a better view.

could be caused by our simplified sampling method. It is interesting to note that the uncertainties of  $f_0$  and  $\dot{f}$  are relatively large for PSR J0337+1715, by factors of  $10^4$ – $10^5$ , when compared with binary pulsars of similar high-quality observations with a comparable span, the number of TOAs, and the timing residual; see e.g., PSRs J0737–3039A [40] and J0348+0432 [41]. The correlations between 16 parameters are plotted in Figure 2 for simulated TOAs with *uniform sampling*. The largest correlation comes from the time of ascending node and the orbital period for the outer orbit which, we suspect, is related to the small number ( $\sim 1.5$ ) of orbital coverage, that makes the variables of the outer orbit likely correlated (see the green  $5 \times 5$  sub-block in Figure 2). The correlation matrices for different noise realizations are hardly distinguishable, and those for *step sampling* are fully consistent with Figure 2.

#### IV. EQUIVALENCE OF MASSES

The discovery of the triple pulsar has triggered some studies in tests of the strong equivalence principle (i.e.  $m_{\mathcal{I}} = m_{\mathcal{P}}$  for self-gravitating bodies) [15, 30]. Preliminary results showed that it probes the difference in  $m_{\mathcal{P}}/m_{\mathcal{I}}$  between NSs and WDs at  $10^{-5}$ – $10^{-8}$  [42, 43]. The Square Kilometre Array will improve that further and limit the scalar-tensor gravity stringently [44]. No detailed analysis has been published yet. Here we perform such a study. In addition to  $m_{\mathcal{I}} = m_{\mathcal{P}}$ , a new test is proposed to study the possibility of  $m_A \neq m_{\mathcal{P}}$ . Because Newton's third law is violated if  $m_A \neq m_{\mathcal{P}}$  [10], it is the first test of the famous *actio = reactio* formalism with strongly self-gravitating bodies.

The two WDs in the triple system are assumed to have a similar strength in violating the equivalence of

<sup>3</sup> <http://dan.iel.fm/emcee>

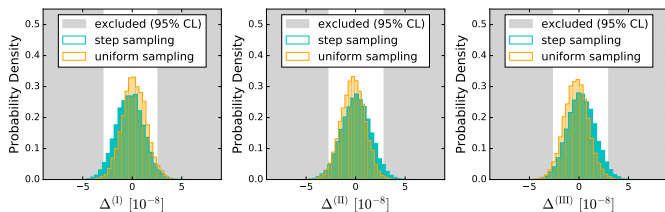


FIG. 4. The *posteriori* PDFs for the equivalence-violating parameters from simulated TOAs with  $\Delta^{(I)} = \Delta^{(II)} = \Delta^{(III)} = 0$ .

masses.<sup>4</sup> The equivalence-violating parameters are defined as,  $\Delta^{(I)} \equiv (m_{\mathcal{A}}/m_{\mathcal{I}})_{\text{NS}} - 1$ ,  $\Delta^{(II)} \equiv (m_{\mathcal{P}}/m_{\mathcal{I}})_{\text{NS}} - 1$ ,  $\Delta^{(III)} \equiv (m_{\mathcal{A}}/m_{\mathcal{I}})_{\text{WD}} - 1$ , and  $\Delta^{(IV)} \equiv (m_{\mathcal{P}}/m_{\mathcal{I}})_{\text{WD}} - 1$ . Corresponding modifications to the gravitational interaction are added to the IAS15 integrator [33, 34], via

$$m_{i,\mathcal{I}} \frac{d^2 \mathbf{r}_i}{dt^2} \equiv m_{i,\mathcal{I}} \mathbf{a}_i = \sum_{j \neq i} -\frac{G m_{i,\mathcal{P}} m_{j,\mathcal{A}}}{r_{ij}^3} \mathbf{r}_{ij}, \quad (1)$$

with  $\mathbf{r}_{ij} \equiv \mathbf{r}_i - \mathbf{r}_j$  and  $r_{ij} \equiv |\mathbf{r}_{ij}|$ . Further analysis shows that one  $\Delta$  can be set to vanish, which is related to an unobservable rescaling. We choose to set  $\Delta^{(IV)} = 0$ . Consequently, the remaining three  $\Delta$ 's should be interpreted as the difference in the mass ratio relative to  $(m_{\mathcal{P}}/m_{\mathcal{I}})_{\text{WD}}$ .

Figure 3 shows examples of the difference in simulated TOAs with the equivalence violation, with respect to TOAs that are simulated with Newtonian gravity. With  $\Delta$ 's of  $10^{-8}$ – $10^{-7}$ , the effects on TOAs are already *much* larger than the achieved timing residual. However, the correlation with orbital elements is strong. In order to assess the true sensitivity of the triple pulsar, a simultaneous fitting of  $\Delta$ 's with other parameters is *necessary*.

We probe the sensitivity of PSR J0337+1715 in constraining  $\Delta$ 's by adding a nonzero  $\Delta$  in the parameter-estimation process. Fake TOAs are simulated as before. Template TOAs are generated with the possibility of allowing a nonvanishing  $\Delta$ . Because of the strong mutual correlations (see Figure 3), we are not able to estimate three  $\Delta$ 's at one time.<sup>5</sup> Instead, they are analyzed separately. 320000 MCMC samples are accumulated for each set of simulated TOAs for each  $\Delta$ . After dropping the first half BURN-IN runs and marginalizing over 16 parameters, we obtain the *posteriori* probability density functions (PDFs) for  $\Delta$ 's. Different noise realizations give consistent results. One example is shown in Figure 4. The region that is excluded by both sampling methods is conservatively taken as the exclusion region. We conclude that, the data quality of PSR J0337+1715 presented in Ref. [30] allows one to constrain  $|\Delta$ 's to

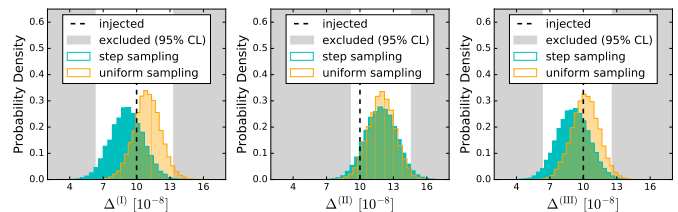


FIG. 5. The recovery of  $\Delta$ 's from simulated TOAs with  $\Delta^{(I)} = 10^{-7}$  (left),  $\Delta^{(II)} = 10^{-7}$  (middle), and  $\Delta^{(III)} = 10^{-7}$  (right).

$\lesssim 3 \times 10^{-8}$ . Because, as seen from Eq. (1), all  $\Delta$ 's modify the trajectories in a similar way, it is not surprising that they are to be constrained with a similar precision.

In addition to *constrain* the equivalence violation in masses, the capability of PSR J0337+1715 to *detect* such violations, if they indeed exist, is also investigated. We *inject* nonvanishing  $\Delta$ 's into our simulated TOAs by modifying the orbital dynamics according to Eq. (1). The same parameter-estimation process by allowing one nonzero  $\Delta$  is performed with these TOAs. The resulting *posteriori* PDFs are shown in Figure 5. As one can see, the equivalence violation can be detected if it indeed exists.

## V. DISCUSSIONS

The equivalence of masses is vital to gravity theories. Already with the *metric theories of gravity* that fulfill the Einstein's equivalence principle [11], three conceptually different masses are distinguishable. For example, in the parametrized post-Newtonian (PPN) formalism [11, 15, 45],

$$\frac{m_{\mathcal{P}}}{m_{\mathcal{I}}} = 1 - \left( 4\beta - \gamma - 3 - \alpha_1 - \frac{2}{3}\zeta_1 - \frac{1}{3}\zeta_2 \right) \frac{E_G}{m_{\mathcal{I}}c^2}, \quad (2)$$

$$\frac{m_{\mathcal{A}}}{m_{\mathcal{I}}} = 1 - \left( 4\beta - \gamma - 3 - 2\zeta_2 - \frac{1}{3}\zeta_1 \right) \frac{E_G}{m_{\mathcal{I}}c^2}, \quad (3)$$

where we have set PPN parameters  $\alpha_2 = \alpha_3 = \xi = 0$ , due to their tight limits ( $10^{-9}$  for  $|\alpha_2|$ ,  $|\xi|$  [46, 47];  $10^{-20}$  for  $|\alpha_3|$  [22]). Using  $E_G/m_{\mathcal{I}}c^2 \simeq 0.1 m_{\text{NS}}/M_{\odot}$  for NSs [48], one constrains  $|4\beta - \gamma - 3 - \alpha_1 - \frac{2}{3}\zeta_1 - \frac{1}{3}\zeta_2|$  and  $|4\beta - \gamma - 3 - 2\zeta_2 - \frac{1}{3}\zeta_1|$  to  $\lesssim 2 \times 10^{-7}$ , with the limits on  $\Delta^{(I)}$  and  $\Delta^{(II)}$  from PSR J0337+1715.<sup>6</sup> Without a fortuitous cancellation,  $\beta$ ,  $\gamma$ ,  $\alpha_1$ ,  $\zeta_1$ , and  $\zeta_2$ , can be constrained to  $\lesssim 10^{-7}$ , improving the current best bounds [15] by  $10^2$ – $10^5$ . Even allowing a fortuitous cancellation, one still improves their bounds, for example, *at least* by  $\gtrsim 10^3$  for  $\zeta_1$ .

With the limit on  $\Delta^{(II)}$ , the Nordtvedt parameter [26],  $\eta_{\text{N}} (= 4\beta - \gamma - 3 - \alpha_1 - \frac{2}{3}\zeta_1 - \frac{1}{3}\zeta_2)$  in the PPN formalism [11]), improves by  $\gtrsim 10^3$  with respect to LLR [20].

<sup>4</sup> It is easy to relax this assumption, but leading to an unnecessary redundancy with little theoretical interests.

<sup>5</sup> Simultaneous fittings with three  $\Delta$ 's are tried, but the convergence is very bad after a long MCMC run.

<sup>6</sup> For this particular analysis,  $\Delta^{(III)}$  can be assumed to vanish, due to the relatively weak gravity of WDs,  $(E_G/m_{\mathcal{I}}c^2)_{\text{WD}} \simeq 10^{-4}$ .

This would be the first time that compact objects provide a tighter limit on  $\eta_N$  than the Solar system. The test of  $m_P = m_A$  would be the first test with strongly self-gravitating bodies, which vastly extends the regime explored by the previous tests in terms of objects' compactness [28, 29]. The test would surpass the best test [29] by  $10^6$  within the post-Newtonian analysis, and would be the first test of Newton's third law with strongly self-gravitating bodies.

We stress that, although our simulated TOAs are able to reproduce major features of the real observation [30], they are simplified compared with the complications in the real data, e.g., the heteroscedasticity in TOAs from different telescopes, the irregular jumps between observing sessions, the remove of time-dependent interstellar dispersion, the correlation with parallax and proper mo-

tion [49]. This study is intended to advocate the program to analyze foundational principles on the equivalence of masses with the remarkable triple system. The analysis in this work is solely based on the observation presented in Ref. [30]. In reality, more data have accumulated since that publication. We urge observers to test the equivalence of masses with real timing data.

## ACKNOWLEDGMENTS

We thank Stanislav Babak, Alessandra Buonanno, Abraham Harte, Vivien Raymond, and Norbert Wex for helpful discussions. The Markov chain Monte Carlo runs were performed on the VULCAN cluster at the Albert Einstein Institute in Potsdam-Golm.

- 
- [1] A. Einstein, *Annalen der Physik* **323**, 639 (1905).
  - [2] A. Einstein, *Annalen der Physik* **354**, 769 (1916).
  - [3] K. Schwarzschild, *Sitz. der Königl. Preuss. Akad. der Wiss. (Berlin)*, 189 (1916).
  - [4] L. de Broglie, *Nature (London)* **112**, 540 (1923).
  - [5] P. W. Higgs, *Rev. Mod. Phys.* **86**, 851 (2014).
  - [6] F. Englert, *Rev. Mod. Phys.* **86**, 843 (2014).
  - [7] ATLAS Collaboration, *Physics Letters B* **716**, 1 (2012).
  - [8] CMS Collaboration, *Physics Letters B* **716**, 30 (2012).
  - [9] E. Wigner, *Annals of Mathematics* **40**, 149 (1939).
  - [10] H. Bondi, *Rev. Mod. Phys.* **29**, 423 (1957).
  - [11] C. M. Will, *Theory and Experiment in Gravitational Physics* (Cambridge University Press, 1993).
  - [12] W. B. Bonnor, *Class. Quantum Grav.* **9**, 269 (1992).
  - [13] N. Rosen and F. I. Cooperstock, *Class. Quantum Grav.* **9**, 2657 (1992).
  - [14] I. Newton, *Philosophiae Naturalis Principia Mathematica* (Streater, London, 1687).
  - [15] C. M. Will, *Living Reviews in Relativity* **17**, 4 (2014).
  - [16] P. Touboul, G. Métris, V. Lebat, and A. Robert, *Class. Quantum Grav.* **29**, 184010 (2012).
  - [17] A. M. Nobili, M. Shao, R. Pegna, and et al., *Class. Quantum Grav.* **29**, 184011 (2012).
  - [18] J. Overduin, F. Everitt, P. Worden, and J. Mester, *Class. Quantum Grav.* **29**, 184012 (2012).
  - [19] P. L. Bender, D. G. Currie, R. H. Dicke, and et al., *Science* **182**, 229 (1973).
  - [20] J. G. Williams, S. G. Turyshev, and D. H. Boggs, *Class. Quantum Grav.* **29**, 184004 (2012).
  - [21] T. Damour and G. Schäfer, *Phys. Rev. Lett.* **66**, 2549 (1991).
  - [22] I. H. Stairs, A. J. Faulkner, A. G. Lyne, and et al., *Astrophys. J.* **632**, 1060 (2005).
  - [23] M. E. Gonzalez, I. H. Stairs, R. D. Ferdman, and et al., *Astrophys. J.* **743**, 102 (2011).
  - [24] P. C. C. Freire, M. Kramer, and N. Wex, *Class. Quantum Grav.* **29**, 184007 (2012).
  - [25] W. W. Zhu, I. H. Stairs, P. B. Demorest, and et al., *Astrophys. J.* **809**, 41 (2015).
  - [26] K. Nordtvedt, *Phys. Rev.* **169**, 1017 (1968).
  - [27] K. Nordtvedt, *Class. Quantum Grav.* **18**, L133 (2001).
  - [28] L. B. Kreuzer, *Phys. Rev.* **169**, 1007 (1968).
  - [29] D. F. Bartlett and D. Van Buren, *Phys. Rev. Lett.* **57**, 21 (1986).
  - [30] S. M. Ransom, I. H. Stairs, A. M. Archibald, and et al., *Nature (London)* **505**, 520 (2014).
  - [31] C. Lämmerzahl, *Fund. Theor. Phys.* **162**, 25 (2011).
  - [32] T. M. Tauris and E. P. J. van den Heuvel, *Astrophys. J. Lett.* **781**, L13 (2014).
  - [33] H. Rein and S.-F. Liu, *A&A* **537**, A128 (2012).
  - [34] H. Rein and D. S. Spiegel, *MNRAS* **446**, 1424 (2015).
  - [35] R. Blandford and S. A. Teukolsky, *Astrophys. J.* **205**, 580 (1976).
  - [36] J. Goodman and J. Weare, *Comm. App. Math. and Comp. Sci.* **5**, 65 (2010).
  - [37] D. Foreman-Mackey, D. W. Hogg, D. Lang, and J. Goodman, *Publ. Astron. Soc. Pac.* **125**, 306 (2013).
  - [38] S. Brooks, A. Gelman, G. L. Jones, and X.-L. Meng, *Handbook of Markov Chain Monte Carlo* (Chapman and Hall/CRC, 2011).
  - [39] A. Gelman and D. Rubin, *Stat. Sci.* **7**, 457 (1992).
  - [40] M. Kramer, I. H. Stairs, R. N. Manchester, and et al., *Science* **314**, 97 (2006).
  - [41] J. Antoniadis, P. C. C. Freire, N. Wex, and et al., *Science* **340**, 448 (2013).
  - [42] W.-b. Han and S.-l. Liao, arXiv:1407.0090 (2014).
  - [43] L. Shao, I. H. Stairs, J. Antoniadis, and et al., *Advancing Astrophysics with the Square Kilometre Array (AASKA14)*, 42 (2015), arXiv:1501.00058
  - [44] E. Berti, E. Barausse, V. Cardoso, and et al., *Class. Quantum Grav.* **32**, 243001 (2015).
  - [45] C. M. Will, *Astrophys. J.* **204**, 224 (1976).
  - [46] L. Shao, R. N. Caballero, M. Kramer, and et al., *Class. Quantum Grav.* **30**, 165019 (2013).
  - [47] L. Shao and N. Wex, *Class. Quantum Grav.* **30**, 165020 (2013).
  - [48] T. Damour and G. Esposito-Farèse, *Class. Quantum Grav.* **9**, 2093 (1992).
  - [49] S. M. Kopeikin, *Astrophys. J. Lett.* **467**, L93 (1996).